2016

Modelling and Preliminary Design of a Variable-BVR Rotary Valve Expander with an Integrated Linear Generator

Sergei Gusev
Ghent University, Belgium, sergei.gusev@ugent.be

Davide Ziviani
Ghent University, Belgium, davide.ziviani@ugent.be

Jasper de Viaene
Ghent University, Belgium, purdueherrickconf16@gmail.com

Stijn Derammeleaere
Ghent University, Belgium, Martijn.vandenBroek@UGent.be

Martijn van den Broek
Ghent University, Belgium

Modelling and Preliminary Design of a Variable-BVR Rotary Valve Expander with an Integrated Linear Generator

Sergei GUSEV[1*], Davide ZIVIANI[1], Jasper DE VIAENE[2], Stijn DERAMMELEAERE[2], Martijn VAN DEN BROEK[1]

[1]Ghent University, Department of Flow, Heat and Combustion Mechanics, Kortrijk, Belgium
[2]Ghent University, Department of Electrical Energy, Systems and Automation, Kortrijk, Belgium
Contact Information: Servei.Gusev@UGent.be

* Corresponding Author

ABSTRACT

The Organic Rankine Cycle (ORC) is currently one of the most suitable technologies to convert waste heat into mechanical work or electricity. While large and medium scale systems are widely available on the market for various temperature and power ranges, small-scale ORCs below 50 kWe are still in a pre-commercial phase because of the relatively high specific cost per kW and the lack of technologically mature and high efficient expanders. Small-scale ORC installations for automotive applications operate at variable heat source profiles combined with the fluctuating power demand from a vehicle. The prediction of an optimum operating point is challenging.

Exhaust gases are a limited heat source, therefore the more heat is recovered at an optimal cycle efficiency level, the more power is produced. By using advanced cycle architectures (e.g. trilateral ORCs, partial-evaporating ORCs, zeotropic mixture ORCs, etc.) and the right fluids, an optimum can be found. An expander with a variable built-in volume ratio (BVR) can allow to operate at optimal conditions within the whole range of pressures imposed by the variable heat source and heat sink. Adjustable expanders are known but mainly limited to large-scale applications. Neither a positive displacement expander, nor a turbine can provide an optimal expansion of a working fluid in a wide range of operation conditions.

As a response to this challenge, the concept of a variable-BVR piston expander with an integrated linear generator is proposed in this paper. The internal part-load control is based on a rotary valve which controls the suction and discharge processes in the expander. An analytic model has been developed to relate the position of the valve with the motion of the piston.

By means of a deterministic model, the influence of the main design parameters is investigated. A preliminary design based on the expander model results is described and the predicted performance over the operating range of interest is discussed.

1. GENERAL DESCRIPTION

1.1 Mechanical design

The proposed expander is shown in Figure 1 and it consists of the following main parts:

1. Stationary cylindrical housing (shown semi-transparent) with wall openings for intake and discharge of the working fluid. Two working chambers are engaged alternately to expand and to discharge the working fluid. These chambers are formed by two stators located at both sides of the housing;
2. Double acting cylindrical piston, coaxial with the housing, consisting of two skirts connected with each other by a central element. The thickness of this element is defined by the pressure difference, which is dependent on the application, in order to ensure the required mechanical resistance. Permanent magnets are embedded in such a way that the control of the rotor by means of two degrees of freedom (rotation and translation) is possible by the coils. The reciprocation of the piston induces electricity, while the rotation controls the intake and discharge

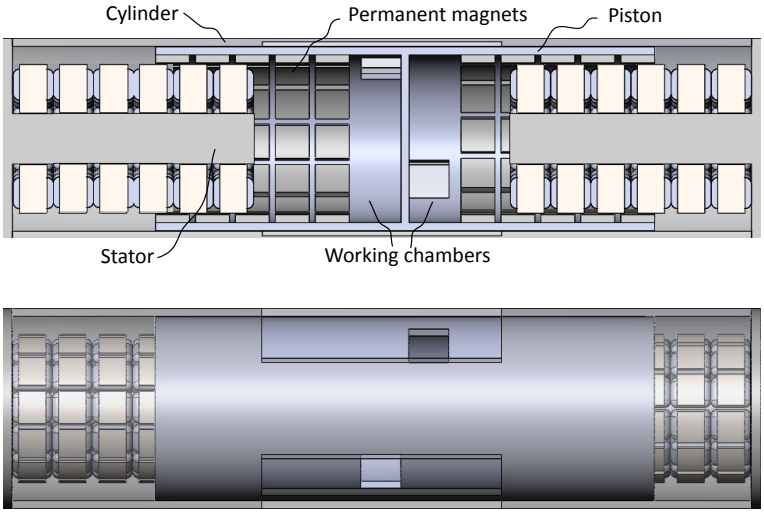

Figure 1: Expander cut-away and with semi-transparent housing

process of the working fluid by opening and closing the intake and the discharge ports. The outer diameter of the piston is matched with the inner diameter of the cylindrical housing with a minimal clearance;

3. Power and control electronics.

1.2 Operation principle

Working chambers are enclosed between the central element, the skirts and the stators. When the piston moves to the right, the volume of the first chamber increases and the volume of the second chamber decreases and vice versa. The skirts with openings act as valves: when the skirt openings converge with the openings in the housing connected to the high pressure side, these openings act as inlet ports. When connected to the low pressure side – as outlet ports. When the skirt opening is not converged with any of the in- and outlet openings of the housing, but facing an inner wall of the cylinder, the working chamber is isolated. Three working phases can identified as function of the piston movement and the angular position: intake, expansion and discharge, which are depicted in Figure 2.

Depending on the piston linear position at the moment of closing of the inlet, the volume V_1 is isolated and further expanded until the volume V_2. The built-in volumetric ratio is defined as:

$$BVR = \frac{V_2}{V_1} = \frac{1}{\chi}, \tag{1}$$

where χ is the piston relative displacement at the moment when the inlet port closes. Figure 3 illustrates the volume ratio of around 10 corresponding to the piston relative displacement of χ=0.1 (position of the right-bottom corner of the skirt opening).

Piston movement is controlled by power electronics for optimal expansion which requires further analysis. In fact, there are no limitations such as volume in function of the crankshaft angle. To adjust the expansion ratio, the intake and the discharge ports are controlled by means of a piston skirt. An additional degree of freedom is added: the piston can rotate closing the intake port quasi at any time independent of the linear position. The volumetric efficiency of such expander is quite high and only defined by machining precision. Ideally, there is no working fluid left in the clearance volume when the piston reaches extreme left or right position. The placement of the in- and outlet ports symmetrically on opposing sides of the cylinder eliminates side forces acting upon the mechanism. The unit can be made fully hermetic with no seals and moving parts except the piston itself.

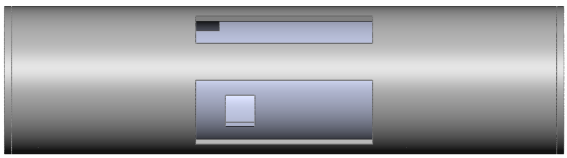

(a) Intake port (smaller port) of the left chamber is open, the piston moves from left to right. Expanded working fluid in the right chamber is discharged to the condenser (wider port).

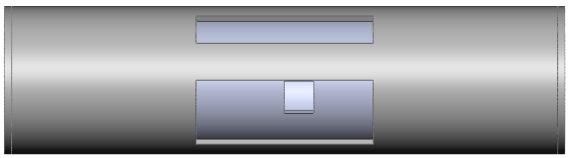

(b) Intake process in the left chamber finishes, the discharge port of the right chamber is still open.

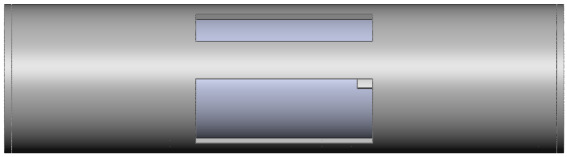

(c) In the left chamber, the expansion starts: the port is closed, the piston keeps moving to the right.

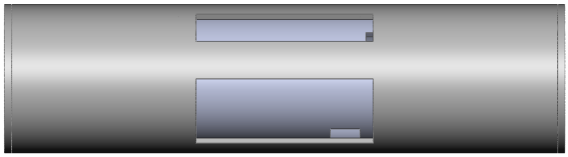

(d) The left chamber is connected to the condenser and the discharge process starts. The function of the chambers alternates, intake process is now started in the right chamber.

Figure 2: Valve operation principle.

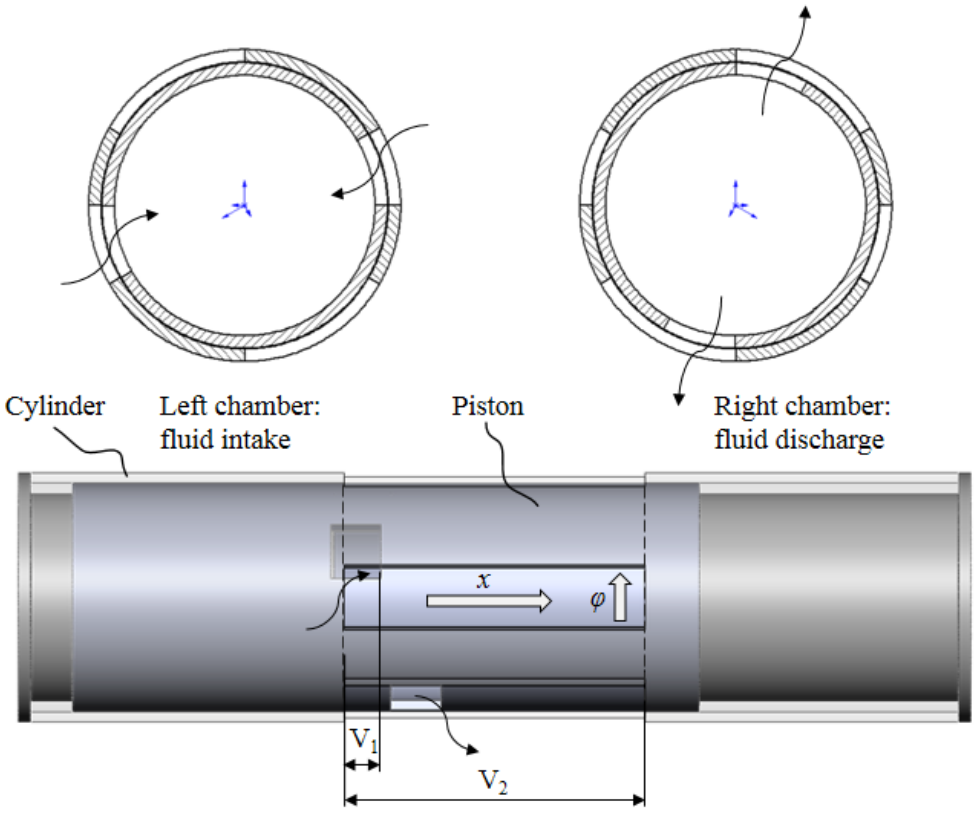

Figure 3: Variable volume ratio

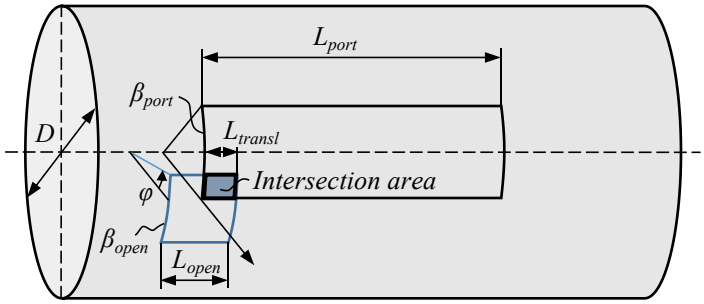

Figure 4: Schematic of the port geometry.

2. THERMODYNAMIC MODEL

An hybrid gray box model adapted from (Glavatskaya et al., 2012) is developed to simulate the expander. The process is split up into infinitesimal steps. In order to calculate the necessary thermodynamic parameters, the CoolProp library connected to Python is used (Bell et al., 2014). Air is chosen as a working fluid in order to avoid complexity at the first stage of the prototype development: leakages in a non-optimized setup are inevitable and the use of expensive working fluids will increase operating costs.

The working process consists of three phases: intake, the inlet pressure assumed constant; expansion, the pressure in the working chamber decreases; discharge, the pressure is equalized with the condenser pressure and remains constant.

2.1 Intake and discharge.

The working medium enters the expander through a rectangular port formed by the openings in the housing and the skirts. This process is modeled as an isentropic expansion. The mass flow rate $\dot{m}$ is dependent on the port area S, the inlet pressure p_{su}, the pressure in the cylinder p_{cyl} and can be calculated using the Fliegner's equation:

$$\dot{m}(t) = C_d \cdot S(t) \cdot \rho_{su} \left(\frac{p_{su}}{p_{cyl}(t)} \right)^{\frac{1}{\kappa}} \cdot \sqrt{\frac{2\kappa}{\kappa - 1} \frac{p_{su}}{\rho_{su}} \left[1 - \left(\frac{p_{cyl}(t)}{p_{su}} \right)^{\frac{\kappa-1}{\kappa}} \right]}. \tag{2}$$

The intersection area is changing according to the rotation and the translation of the piston (Figure 4). Depending on the pressure ratio across the inlet port, the discharge coefficient C_d from 0.5 to 0.9 is interpolated from the Figure 5 of (Novák & Koza, 2013).

The position of the lower left corner of the cylinder wall opening is chosen as the reference point. The start of the intake process corresponds with the position of the piston when the lead-top corner of the skirt opening is at the reference point. A simplified algorithm defining the overlap of two rectangular openings is used to calculate the intersection area:

$$\begin{aligned} S(t) = &\left(max(0, min(L_{transl}(t), L_{port}) - max(0, L_{transl}(t) - L_{open})\right) \times \\ &\times \left(max(0, min(\varphi(t), \beta_{port}) - max(0, \varphi(t) - \beta_{open})\right) \cdot \frac{\pi D}{2} \cdot n\,, \end{aligned} \tag{3}$$

where n is the number of ports. In current configuration, two axisymmetric ports are used.

A similar model is applied to estimate the mass flow rate during the discharge process. The corresponding pressures p_{cyl} and p_{dis} are used.

2.2 Expansion.

The expansion process is simulated as a sequence of small steps: an isentropic expansion, isochoric heating by friction, the heat transfer from or to the expander walls. The last process is described by a Newtonian model:

$$\dot{Q}_{cyl}(t) = h(t) \cdot A_p(t) \cdot (T_{cyl}(t) - T_p) . \tag{4}$$

In literature, different correlations for the in-cylinder heat transfer coefficient *h* are available, for example: the Eichelberg correlation (Eichelberg, 1939), the Woschni correlation (Woschni, 1967) and the Hohenberg correlation (Hohenberg, 1979). These correlations applied to a high stroke/diameter ratio reciprocating engine have been compared by Fula et al. (2013). The Woshini correlation have been selected and it is given by:

$$h(t) = 3.26 D^{-0.2} \left(\frac{p_{cyl}(t)}{10^5} \right)^{0.8} T_{cyl}(t)^{-0.55} \left(\frac{dx}{dt} \right)^{0.8} . \tag{5}$$

The piston surface temperature is assumed as the average between the in- and the outlet gas temperatures.

$$T_p = \frac{T_{su} + T_{dis}}{2} . \tag{6}$$

This temperature can be adjusted if a water cooling system is used.

2.3 Leakage flow

The leakage flow is dependent on the pressure difference and the gap size between the piston and the cylinder walls. Since the goal of the current study is to optimize the dynamic behavior of the expander, a relatively high leakage flow is permitted in order to minimize the friction forces. The exact flow will be measured during static tests and subtracted from the final results.

3. THE EQUATION OF MOTION

The model of the free-piston expander is developed as suggested by Mikalsen & Roskilly (2008). Since the rotation and translation of the piston have to be synchronized, the model is focused on the accurate definition and control of the piston position in both dimensions. The dynamics of the piston is defined by the Newton's second law.

$$F_{p,cyl} - F_{p,dis} - F_{fr} - F_{el} = m_p \frac{d^2x}{dt^2} , \tag{7}$$

where $F_{p,cyl}$ and F_{dis} are gas forces in the left and right working chambers respectively during the piston motion from left to right. Both gas forces are applied to the same central element and are opposing each other.

The friction force F_{fr} depends on the piston speed, which is the vector sum of the translation and the rotational speeds of the piston. The dynamic friction behaviors of pneumatic cylinders based on the LuGre model is studied in (Tran & Yanada, 2013). The results obtained in this study are used for the simplified friction force correlation for the free-piston model. Due to a continuous rotation of the piston, the resulting speed is non-zero at the extreme piston positions. Therefore, the Stibeck-effect at near-zero speeds can be neglected and a linear dependence of the friction force from the speed can be used.

The electromagnetic force F_{el} applied to the piston is adjusted during the piston motion in order to stop the piston at its extreme left and right positions, so all kinetic energy is absorbed and transformed into electricity. The approach is similar to (Petrichenko et al., 2015). The resulting equation can be written as follows:

$$F_{el}(t) = \frac{\pi D^2}{4} (p_{cyl}(t) - p_{dis}) - F_{fr} \left(\frac{dx}{dt} \right) - m_p \frac{d^2x}{dt^2} . \tag{8}$$

The Equation 8 is used to control the drive of the linear motor, the position sensor is used for the feedback of the piston position.

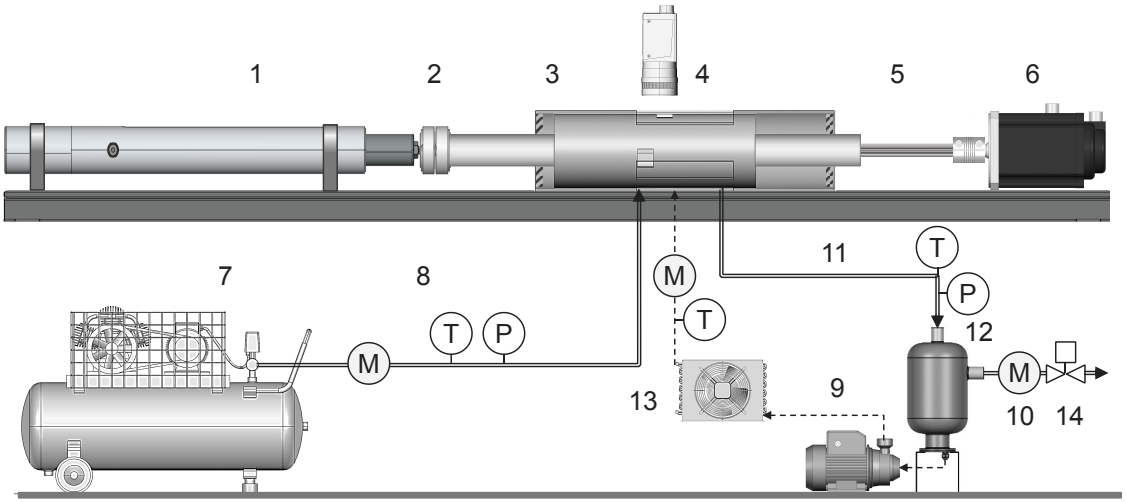

Figure 5: Test setup

4. TEST SETUP

The key feature of this setup is the ability to control both the rotation and translation of the piston. The layout of the setup is shown in Figure 5. While the final goal is a fully integrated system, for convenience and feasibility during the proof of concept phase, both movements are designed to be controlled by a different electromechanical actuators.

4.1 Main Components

The test setup consists of: a linear generator with an integrated position sensor (1) connected to the expander (3) through a coupling (2) transferring only the linear motion and preventing the generator shaft from rotation. The other side of the expander is connected to a servo motor with an encoder by means of a spline shaft (5) which insures the right angle positioning while the expander shaft can freely slide along it.

The expander is driven by compressed air provided by an air compressor unit (7). Temperature (T), pressure (P), and mass flow meters (M) are placed on the air supply line in order to determine the input power.

To ensure the lubrication and the sealing of the expander, an oil injection system is placed. It consists of a circulation pump (9), an oil separator (10) and a cooler (13) to reject the heat produced by friction.

The second flow meter is placed at the air discharge line (12) to measure the leakage flow by calculating the difference between the first flow meter placed at the inlet of the expander. The outlet pressure is controlled by a motorized throttling valve (14) to set up any desired pressure.

A high speed camera (4) is used to observe the inlet port operation.

4.2 Expander sizing

The sizing of the expander for the setup depends on the linear generator available. Since linear generators are still rare on the market, a linear motor operating in a brake mode is found, which fits the requirements. Basing on the characteristics provided by the manufacturer, the maximal static force applied to the generator is 5.18 kN. The nominal inlet pressure of 1 MPa is chosen. These parameters define the diameter of the piston. The speed and the force relationship is dependent on the linear generator used and provided by the manufacturer. This dependence is acquired into the model. The major setup parameters are summarized in Table 1.

Table 1: Main parameters of the designed test setup

Bore (m)	Stroke (m)	Frequency (Hz)	Moving mass (kg)	Volume flow (nm^3/sec)	Inlet pressure (Pa)	Discharge pressure (Pa)
0.08	0.31	5.0	40	0.016	10^6	10^5

5. RESULTS AND DISCUSSIONS

The developed model dictate the rotational movement in line with the linear movement of the expander. The speed and the acceleration of both movements can be controlled independently. In order to lower the pressure loss at the inlet, the linear speed can be kept as low as possible, while during the expansion process the linear movement can be optimized for a maximal power output.

The frequency is kept constant and the electrical force is varied in order to find the maximal achievable stroke length and the maximum power output conditions. The major results of the simulation of the expansion are shown on the Figure 6.

From the simulations it is cleared out that the piston should be forced to move at the beginning of the expansion process as it is shown on Figure 6(a) otherwise it will not be able to reach the maximum speed related to the current electromagnetic force applied (Figure 6(d)). As a result, a much smaller stroke length will be required for the same frequency (Figure 6(c)), which in combination with the diameter of the piston and the working frequency define the swept volume of such an expander and the mass flow rate through the system. The lower mass flow rate will cause a lower power output.

During the market survey, some important limits were figured out. The speed is in close relationship with the moving mass of the translator, which is typically assembled from a number of magnetic elements, and the power applied to the coils. Linear motors, characterized by a high-dynamic behavior, are not able to hold a certain position if a high static force is applied. This is the case at the beginning of the intake process when the piston is exposed to the inlet pressure, which is expected to be relatively high in the target applications. The cycle of acceleration / deceleration is chosen accordingly to the characteristics of the motor available (Figure 6(f)). The resulting average accelerating and the power output are shown on Figure 6(e). The electromagnetic force profile is chosen to be constant for the first simulations but it can be further optimized to allow the generator operate at maximal efficiency.

As it can be seen on Figure 6(b), the pressure drop over the inlet valve is relatively small at the beginning of the intake but at the end it becomes higher. An optimization of the piston rotational speed profile is needed in order to keep the inlet port open as long as it possible.

6. CONCLUSIONS

The dynamics of the piston must be optimized accordingly to the linear generator used. There is a trade-off between the high dynamics of the piston movement and a relatively high static force typical for the piston extreme positions. The crucial requirement is that the piston position must be controlled by the generator electronics at any moment.

The major difference with the most systems studied is that in the current setup the piston is not freely moving but, instead, its movement is fully controlled, so there are no bouncing devices needed. This approach provides potentially a more efficient way to transform the energy of the expanded gas into electricity since irreversibilities in bouncing devices are avoided.

This setup has the advantage of testing various expanders with different sizes, by easily replacing generators and motors to study the dynamics of the whole system. The piston movement can be matched with the maximum efficiency range of the generator used.

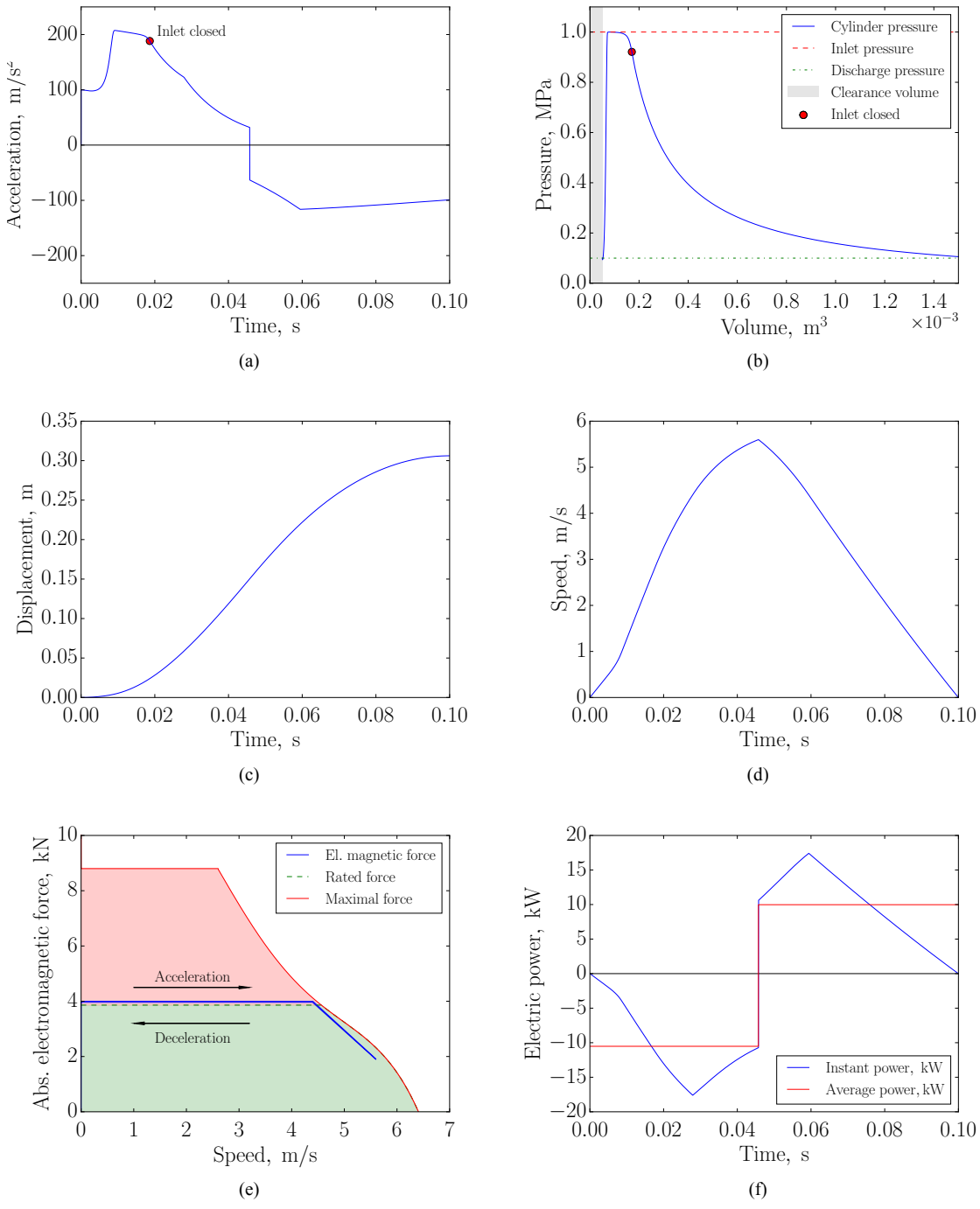

Figure 6: Expansion process.

NOMENCLATURE

A	suface area	(m^2)
C_d	discharge coefficient	(-)
D	diameter	(m)
F	force	(N)
h	heat transfer coefficient	(W/m^2 K)
L	length	(m)
m	mass	(kg)
$\dot{m}$	mass flow rate	(kg/s)
n	number of ports	(-)
p	pressure	(Pa)
$\dot{Q}$	heat flow rate	(W)
S	intersection area	(m^2)
T	temperature	(K)
t	time	(s)
V	volume	(m^3)
x	displacement	(m)

Greek

β	port angle	(rad)
Δ	difference	(-)
κ	isentropic coefficient	(-)
υ	speed	(m/s)
φ	angle of rotation	(rad)
χ	relative displacement	(-)

Subscript

cyl	cylinder
dis	discharge
el	electromagnetic
fr	friction
max	maximal
min	minimal
open	opening
p	piston
port	port
rot	rotation
su	supply
theor	theoretical
transl	translation

REFERENCES

Bell, I. H., Wronski, J., Quoilin, S., & Lemort, V. (2014). Pure and pseudo-pure fluid thermophysical property evaluation and the open-source thermophysical property library coolprop. *Industrial & engineering chemistry research*, *53*(6), 2498–2508.

Eichelberg, G. (1939). Some new investigations on old combustion engine problems. *Engineering*, *148*, 463–446 et 547–560.

Fula, A., Stouffs, P., & Sierra, F. (2013). In-cylinder heat transfer in an ericsson engine prototype. *Renewable Energy and Power Quality Journal, ISSN 2172-038 X*(11).

Glavatskaya, Y., Podevin, P., Lemort, V., Shonda, O., & Descombes, G. (2012). Reciprocating expander for an exhaust heat recovery rankine cycle for a passenger car application. *Energies*, *5*(6), 1751.

Hohenberg, G. (1979). Advanced approaches for heat transfer calculations. *SAE Special Publications*, *SP-449*, 61–79.

Mikalsen, R., & Roskilly, A. (2008). The design and simulation of a two-stroke free-piston compression ignition engine for electrical power generation. *Applied Thermal Engineering*, *28*(5–6), 589–600.

Novák, O., & Koza, V. (2013). Measuring a discharge coefficient of an orifice for an unsteady compressible flow. *Fuels*(1), 21–25.

Petrichenko, D., Tatarnikov, A., & Papkin, I. (2015). Approach to electromagnetic control of the extreme positions of a piston in a free piston generator. *Modern Applied Science*, *9*(1), 119–128.

Tran, X. B., & Yanada, H. (2013). Dynamic friction behaviors of pneumatic cylinders. *Intelligent Control and Automation*, *4*(2).

Woschni, G. (1967). A universally applicable equation for the instantaneous heat transfer coefficient in the internal combustion engine. *SAE*(670931).